Shipboard Meteorological Sensor Comparison: ICEALOT 2008

Daniel E. Wolfe and Laurel K. ThomasArrigo

Meteorological Measurements made from ships are always challenging not only because of the marine environment, but because there are so many different types of instrumentation to choose from. Having a reliable standard set of instruments for the basic measurements of temperature (T), relative humidity (RH), pressure (P), winds (Wsd), precipitation (Pr), and incoming radiation (incoming long and short-wave: LW, SW) was the main purpose of the Improved Meteorological (IMET) system (Hosom et al., 1995) currently in use on most National Oceanic and Atmospheric Administration (NOAA) and Woods Hole Oceanographic Institute (WHOI) research vessels. It is only logical as technology improves to consider changes to these instruments therefore increasing their reliability and accuracy. It is critical to conduct real-world inter-comparison before making any changes. These comparisons provide a smooth transition between sensors and an understanding not only of the accuracies, but of their operating characteristics in the often harsh marine environment.

One of NOAA's Climate Program Office (OCO) goals is high resolution climate data from research and volunteer observing ships. This project involves the development of a roving standard flux measuring system and measurement of direct high-resolution air-sea fluxes on two cruises per year. This system is to be deployed on a series of NOAA and UNOLS research vessels to promote the improvement of climate-quality data from those platforms. Because buoys and most ships and satellites rely on bulk methods to estimate fluxes, another aspect of this project is the use of direct measurements to improve the NOAA/COARE bulk flux algorithm (Fairall and Bradley, 2006, Fairall et al., 2008). Recommendations from the Workshop on High-Resolution Marine Meteorology, COAPS Report 03-01, Florida State University, pp38) identified three important issues to be addressed with the NOAA air-sea observation system:

1. the need to a data quality assurance program to firmly establish that the observations meet the accuracy requirements,
2. a need for observations at high time resolution (about 1 minute),
3. a need to more efficiently utilize research vessels including realizing their potential for the highest quality data and their potential to provide more direct and more comprehensive observations.

For seasonal time scales the net air-sea flux (sum of 5 flux components) needs to be constrained within 10 Wm-2 . Buoys and VOS systems must operate virtually unattended for months, so considerations of practical issues (e.g., power availability, ruggedness, or safe access) are balanced against inherent sensor accuracy and optimal sensor placement. As discussed above, an important function of the in situ measurements is to provide validation data to improve NWP and satellite flux fields. Here, high time resolution and more direct observations can be invaluable for interpreting surface flux measurements and diagnosing the source of disagreements; such information can be provided by suitably equipped RV's. Thus, the accuracy of buoy and VOS observations must be improved and supplemented with high-quality, high time resolution measurements from the US Research Vessel fleet (which is presently underutilized). The necessity for both high time resolution and high accuracy places extreme demands on measurements because some sources of error (such as the effect of ship flow distortion on wind speed) tend to average out over a large sample. To accomplish this will require a careful intercomparison program to provide traceability of buoy, VOS, and RV accuracy to a set of standards.

The International Chemical Experiment in the Arctic Lower Troposphere (ICEALOT 2008) provided an opportunity to inter-compare three different meteorological sets of sensors: the Improved Meteorological (IMET) system, the Vaisala Weather Transmitter WXT510 (WXT), and the Physical Science Division (PSD) Flux Standard (FLUX). The research cruise was broken up into two legs. The first leg started March 19, 2008 (Year Day 79) just north of Boston, MA crossing the North Atlantic to the coast of Norway ending with a short stop in Tromso, Norway April 12, 2008 (Year Day 102). The second leg continued north towards the ice pack, reaching 80^{o} N before heading south as close to the Greenland coast as ice conditions would allow arriving in Reykjavik, Iceland April 23, 2008 (Year Day 114).

All three sets of sensors were mounted on the forward mast of the Research Vessel Knorr (Fig. 1). Tables 1-3 list specifications for the 3 sets of sensors. Some of the major differences between these three systems are the how the winds and precipitation are measured. For the winds, IMET uses a prop-vane while the WXT510 is a 2-axis sonic anemometer and the FLUX a 3-axis sonic anemometer: mechanical (propeller-vane) versus acoustic sampling (sonics). For precipitation, IMET is a self-siphoning rain gauge while the WXT uses the acoustic signal intensity from falling drops with larger drops generating a larger signal, and the FLUX has an optically based sensor.

Figure 1 shows a port-side view of the Knorr with the forward mast lowered and Fig. 2 shows the forward mast raised for sampling. Figure 3 is two expanded views of the forward mast. As with land based meteorological stations, knowledge about the location of sensors is critical in interpreting the data. An additional complication for ship-board systems is the fact the platform on which your sensors are mounted is constantly moving in 3-D. Figures 4-8 illustrates some of the conditions encountered during ICEALOT. Daily time-series and comparison plots from the entire cruise can be found in Appendix A.

For the following comparisons, all the data have been interpolated to a common 1 min time grid. Known bad periods by a particular sensor are not included in the comparison.

Table 1. IMET Sensors

Measurement	Sensor Type	Manufacturer Model	Resolution	Accuracy
Wind Speed	Propeller	RM Young 5305	.1 ms^{-1}	.2 ms^{-1}
Wind Direction	Vane	RM Young 5305	.1 degree	1.4 degree
Air Temperature	RTD*	Rotronic MP-100	.01 degree	±.2 C^o
Relative Humidity	capacitance	Rotronic MP-100	.1 %	±2.7 %
Pressure	DB-1A	DB-1A	.1 mb	.1 mb
Rain Rate Accumulation	Capacitance	RM Young 50202	1 mm	.1 $mmmin^{-1}$
Downwelling shortwave radiation	Pyranometer	Eppley PSP	.4 Wm^{-2}	±1%
Downwelling longwave radiation	N/A	N/A	N/A	N/A
Sea Surface Temperature	Thermistor	OTM-S-212	.1 degree	.1 degree

*Resistance temperature recorder

Table 2. WXT510 Sensor

Measurement	**Sensor Type**	**Manf Model**	**Resolution**	**Accuracy**
Wind Speed	Sonic 2-D	Vaisala WINDCAP	.1 ms^{-1}	+-.3 ms^{-1}
Wind Direction	Sonic 2-D	Vaisala WINDCAP	1^{o}	$.1^{o}$
Air Temperature	RTD*	Vaisala THERMOCAP	$.1^{o}C$	+-$.3^{o}C$ -50^{o} to $20^{o}C$
Relative Humidity	capacitance	Vaisala HUMICAP	.1 %	+-3 % 0-90% +-5% 90-100%
Pressure	DB-1A	Vaisala BAOCAP	.1 mb	.5 mb
Rain Rate Accumulation	Acoustic	Vaisala RAINCAP	 .1 $mmhr^{-1}$ .01 mm	5%

Table 3. PSD Flux Standard

Measurement	Sensor Type	Manf Model	Resolution	Accuracy
Wind Speed	Sonic 3-D	Gill WindMaster Pro	.01 ms^{-1}	±1.5% 0-30ms^{-1} ±3% 30-60ms^{-1}
Wind Direction	Sonic 3-D	Gill WindMaster Pro	.1°	±2° 0-30 ms^{-1} ±3° 30-60 ms^{-1}
Air Temperature	capacitance	Vaisala HMP 235	.1°C	±0.1°C
Relative Humidity	capacitance	Vaisala HMP 235	.1 %	±1 % 0-90% ±2% 90-100%
Pressure	capacitance	Vaisala PTB220	.04 mb	±0.15 hPa
Rain Rate Rate Accumulation	optical	OSI Optical rain	.1 $mmhr^{-1}$ .01 mm	5% accumulation
Downwelling shortwave radiation	pyranometer	Eppley PSP	.4 Wm^{-2}	2-3%
Downwelling longwave radiation	pyrgeometer	Eppley PIR	.1 Wm^{-2}	±1%
Sea Surface Temperature	Thermistor	YSI 46004	.1°C	±.1°C
Motion x, y, z	accelerometer	BEI	.004°s^{-1}	

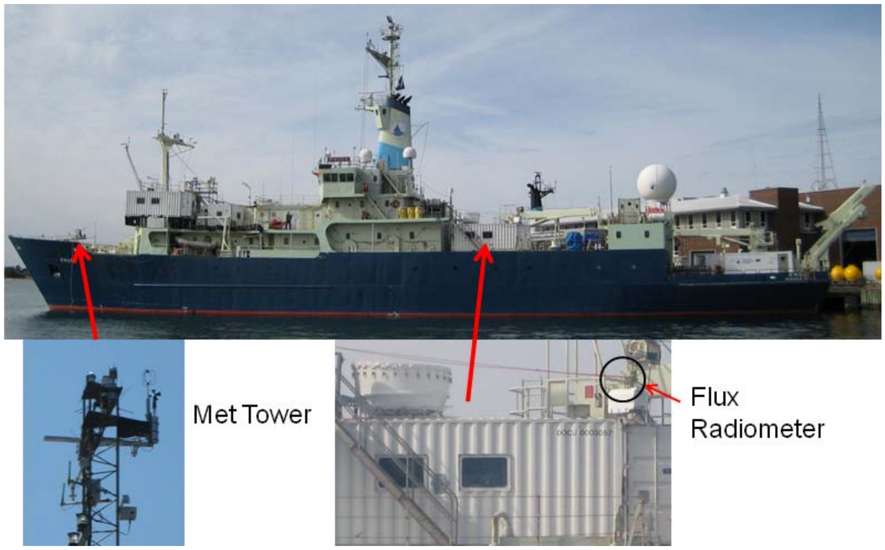

Figure 1. Port-side view of Knorr showing forward meteorological tower and FLUX radiometer locations. Note: Mast is lowered down into position for instrument mounting in this picture.

Figure 2. Tower sensors located on the forward mast on the bow of the Kno

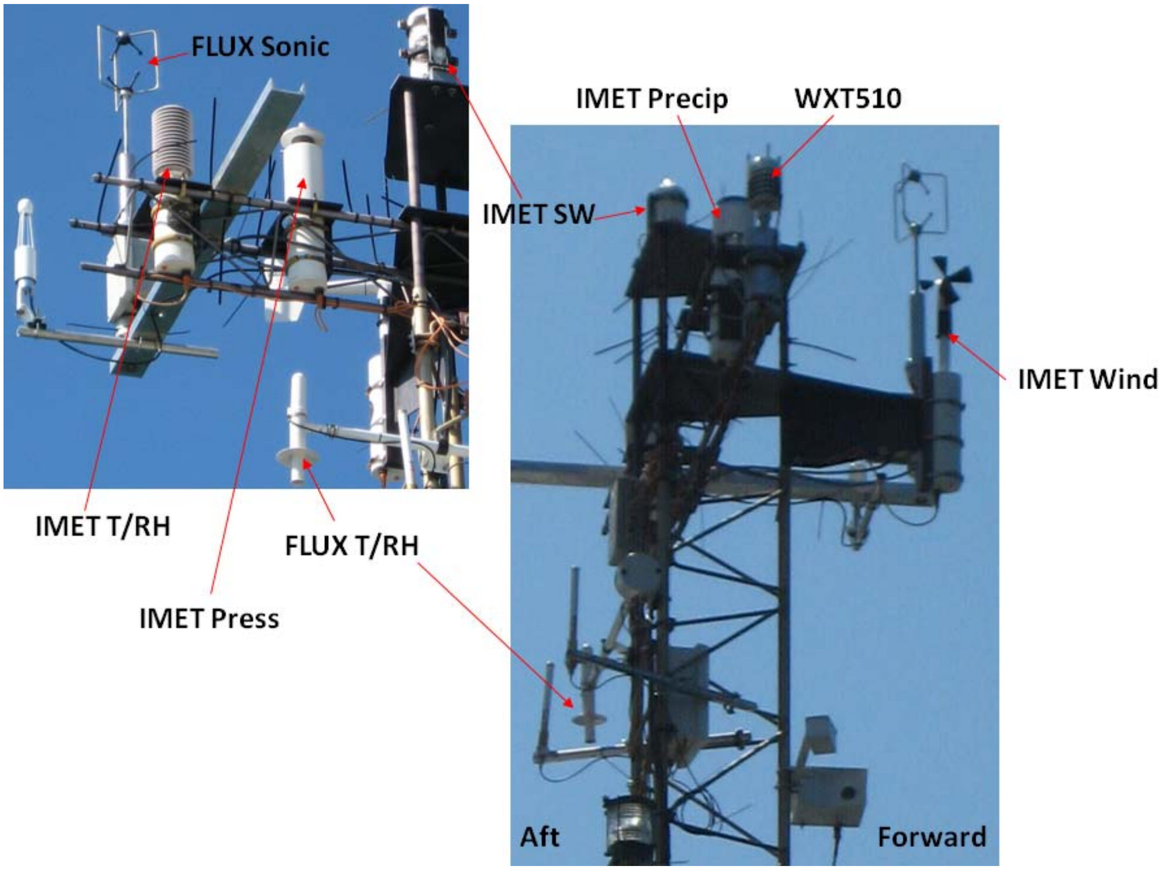

Figure 3. Expanded views of forward mast on the bow of the Knorr. The left image is the port-side sensors viewed from behind looking forward and the right image is looking from the starboard side with the bow to the right.

Figure 4. Map of ICEALOT cruise track starting in Boston, MA Mar 19 and ending in Reykjavik, Iceland Apr 24th

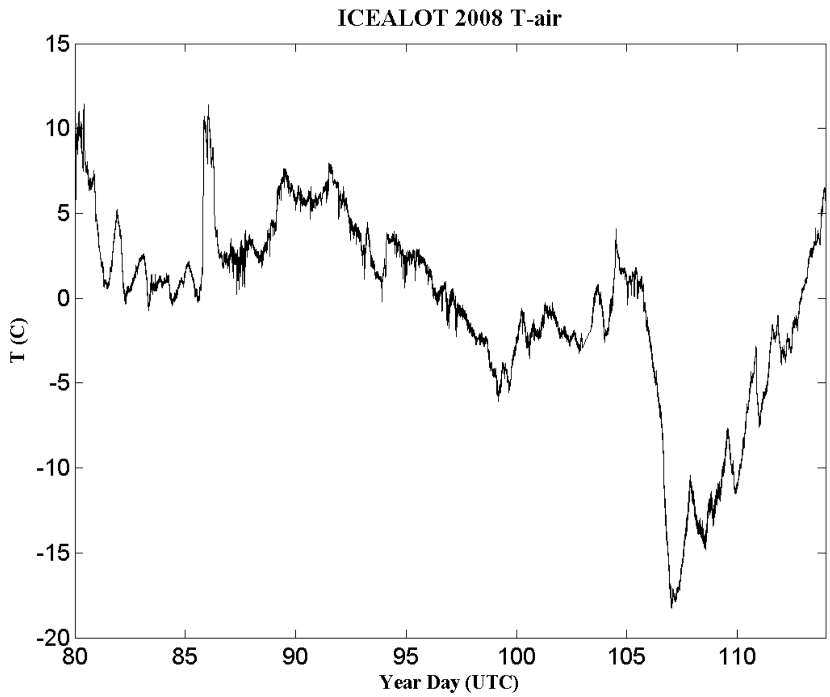

Figure 4. Time series of temperature for entire cruise.

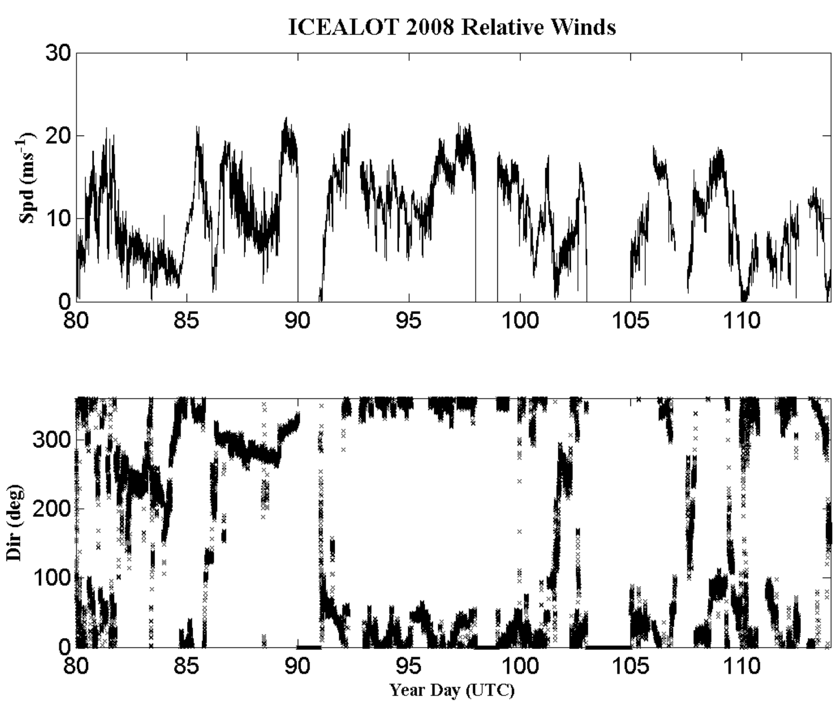

Figure 8. Time series of relative wind speed and direction for entire cruise.

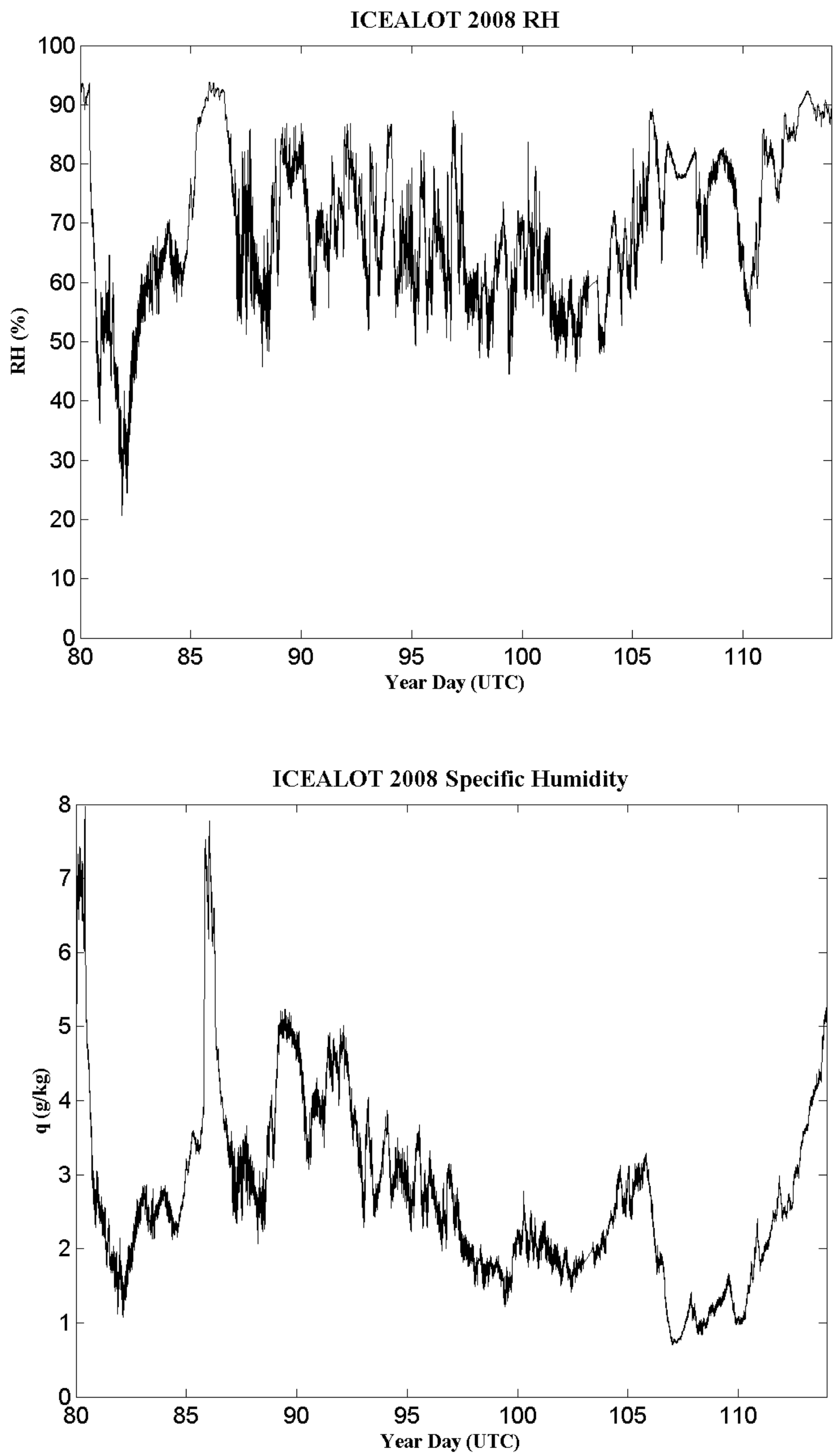

Figure 5. Time series of relative and specific humidity for entire cruise.

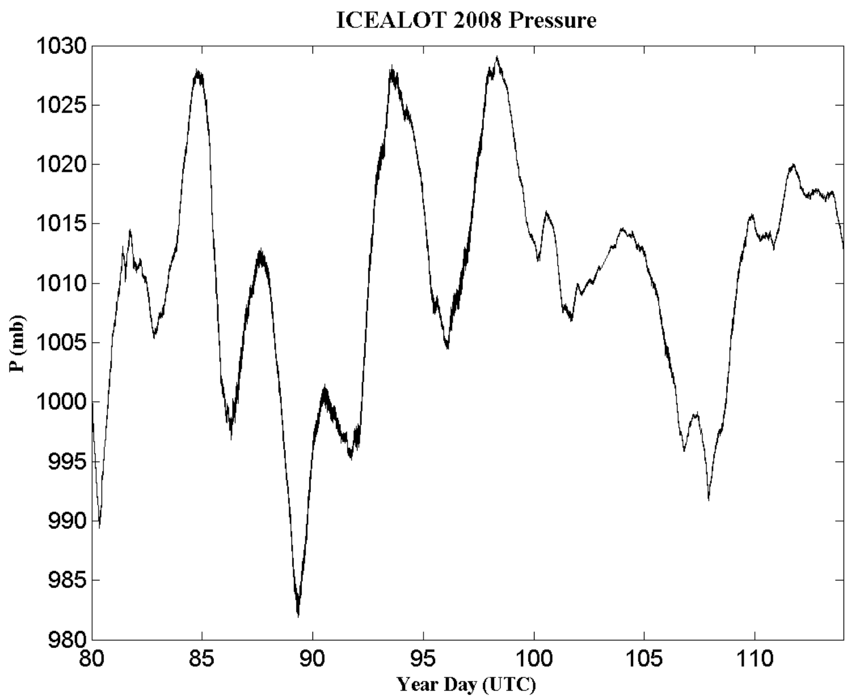

Figure 6. Time series of pressure for entire cruise.

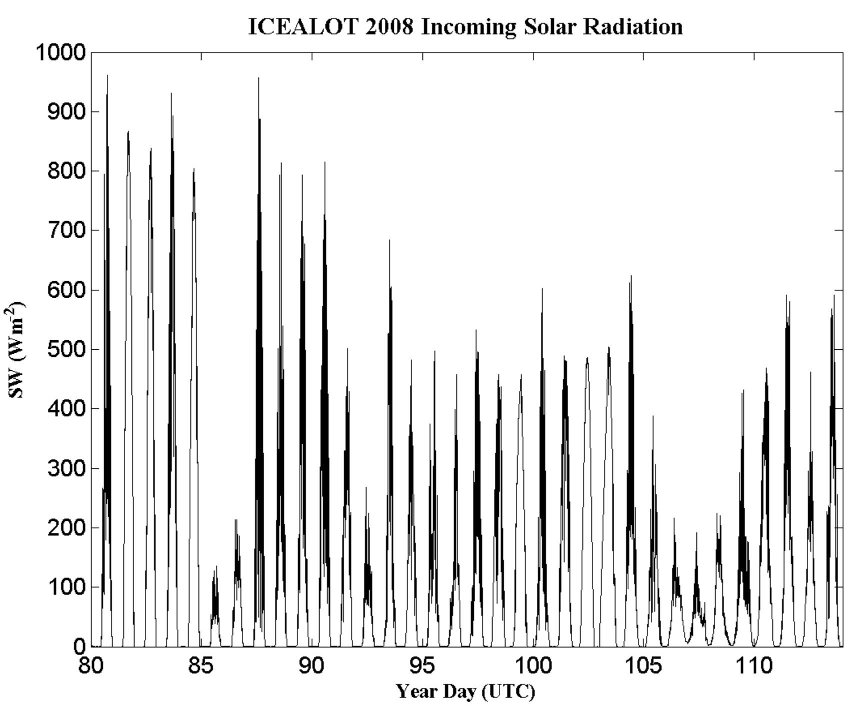

.

Figure 7. Time series of incoming short-wave radiation for entire cruise.

IMET R.M Young Propeller-Vane   Vaisala WXT 520   Gill WindMaster Pro Sonic Anemometer

Figure 9. Three wind sensors

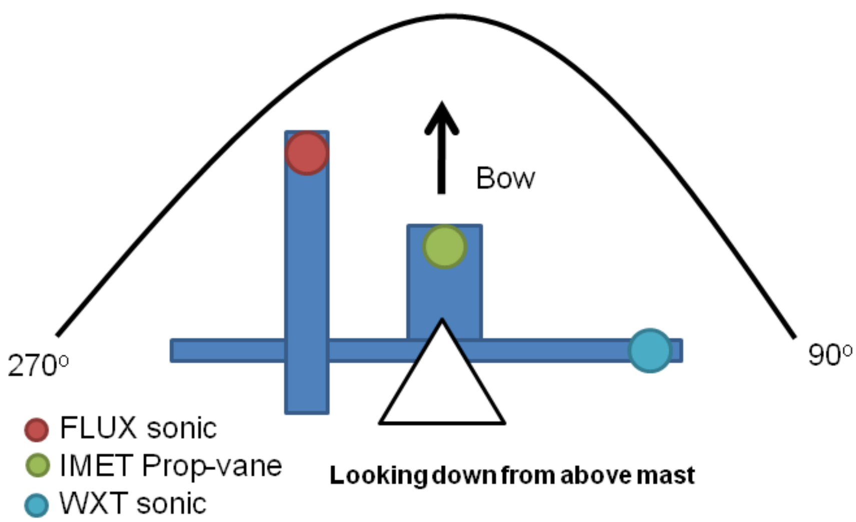

Figure 10. Relative positioning of three wind sensors looking down from above.

Winds:

Figure 9 is a picture of each wind sensors and Fig. 10 a schematic as if you were above the mast looking down. Each wind sensor has a unique fetch for unblocked winds. Placing the wind sensor as high and as far forward as possible creates the least contamination by flow distortion within the 270^{o} to 90^{o} sector relative to the bow. When there is more than one wind sensor, each sensor may compromise the other to some degree. In this instance the FLUX sonic is the highest (Fig. 3) and therefore should have the largest region of uncontaminated winds with the WXT sonic in what appears to be the most compromised location. Figures 11&12 are comparisons of the relative winds between the 3 different sensors. Table 4 lists the statistics for each and Table 5 the correlation between the three sensor components.

Table 4. Relative wind component statistics

Rel u (+fm bow)

	Mean	Min	Max	STD
1 IMET	6.386	-9.350	21.454	6.494
2 WXT	7.483	-14.559	24.787	7.972
3 FLUX	6.587	-15.773	25.253	7.406

Rel-v (+ fm starboard)

	Mean	Min	Max	STD
1 IMET	-0.256	-17.444	18.643	6.928
2 WXT	-1.679	-18.026	19.963	6.535
3 FLUX	-1.225	-24.075	23.993	7.640

Table 5. Relative wind component correlations

Rel u (+fm bow)

	1 vs 2	1 vs 3	2 vs 3
1 IMET	.969	.974	
2 WXT	.970		.972
3 FLUX	.974	. 972	

Rel-v (+ fm starboard)

	1 vs 2	1 vs 3	2 vs 3
1 IMET	.928	.949	.972
2 WXT	.949		.954
3 FLUX	.972	.954	

The wind roses and histograms in Fig 11 show the relative winds for all 3 sensors. When the ship is traveling from place to place, there is no guarantee where the relative wind will be coming from. Once the ship is on station it can be pointed bow first into the wind. As depicted in the wind roses (Fig. 11) the relative wind was predominately coming towards the bow and the best possible angle for all mast mounted sensors. The most obvious difference is that the maximum wind speed for the IMET (propeller-vane) is 3-4 ms^{-1} less than the WXT or FLUX. It is possible this is due to the mechanical nature of the propeller-vane. In terms of relative wind direction, the IMET and FLUX appear more similar with directions centered on North while the WXT is slightly skewed to the west of North. Possible reasons for this could be the location of the WXT such that the winds are deflected more by some of the surrounding instruments and tower structure (Fig 3) or that the initial WXT orientation is off. Analyzing Fig. 12 and Table 5, again we see extremely good correlation between all three sensors. The horizontal scattering artifact seen when comparing FLUX and IMET to the WXT for both components is explained caused by low wind winds from the WXT (Fig. 13). For an unknown reason the WXT produces unrealistic variability at times compared to the other 2 sensors. Even though the log book reports some riming on April 15, it is not obvious why the FLUX sensor, also a sonic, wouldn't be affected too. Other days similar to Fig 14. also point to periods of increase variability and even some spiking in the WXT that again is not evident in the FLUX sensor data. Both the FLUX and WXT had slightly larger STD than the IMET, which is expected with sonic anemometers compared to a propeller-vane. Reviewing all the data there is some indication that the WXT started to have more problems on the second leg when there were colder temperatures and periods of riming.

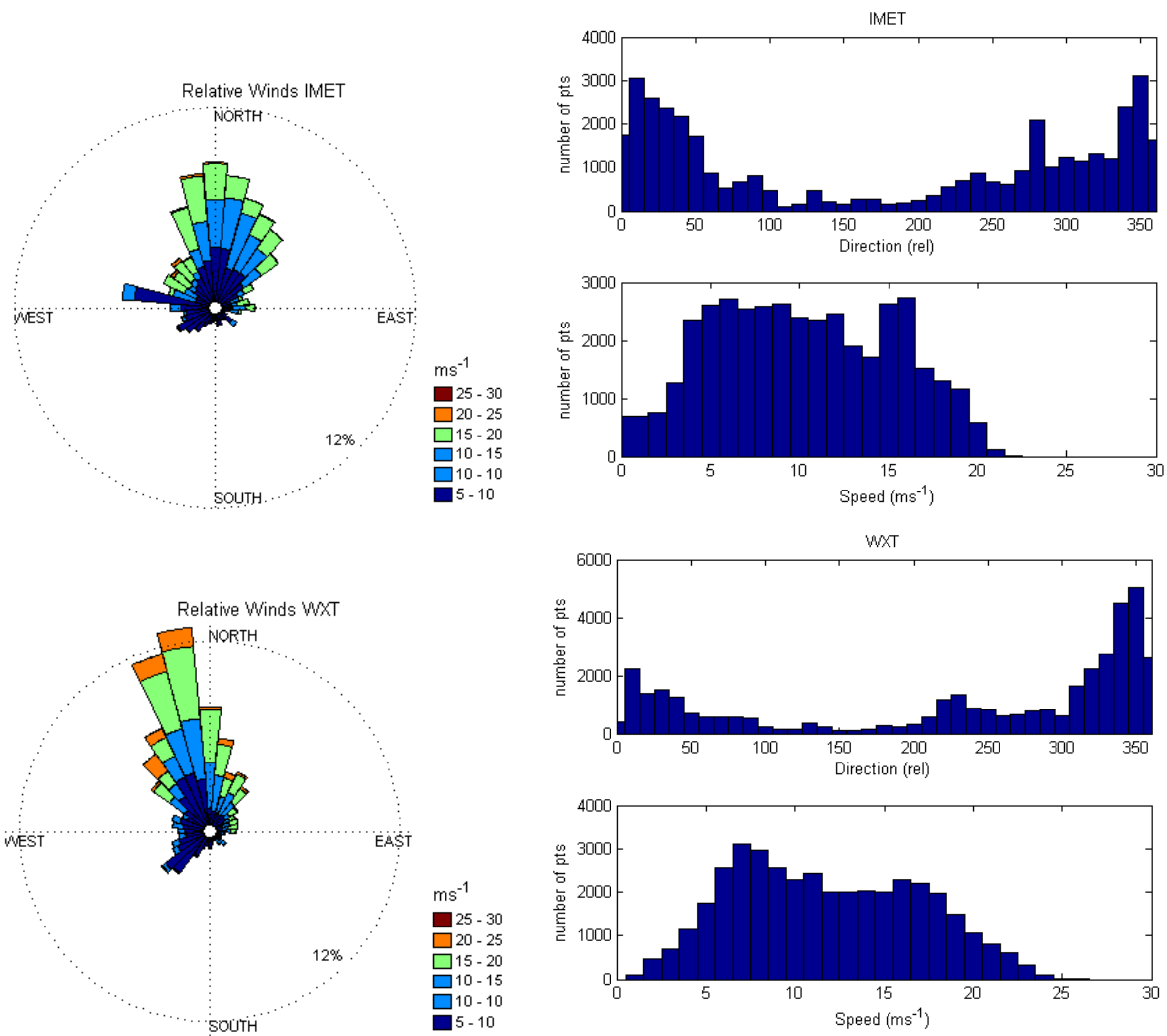

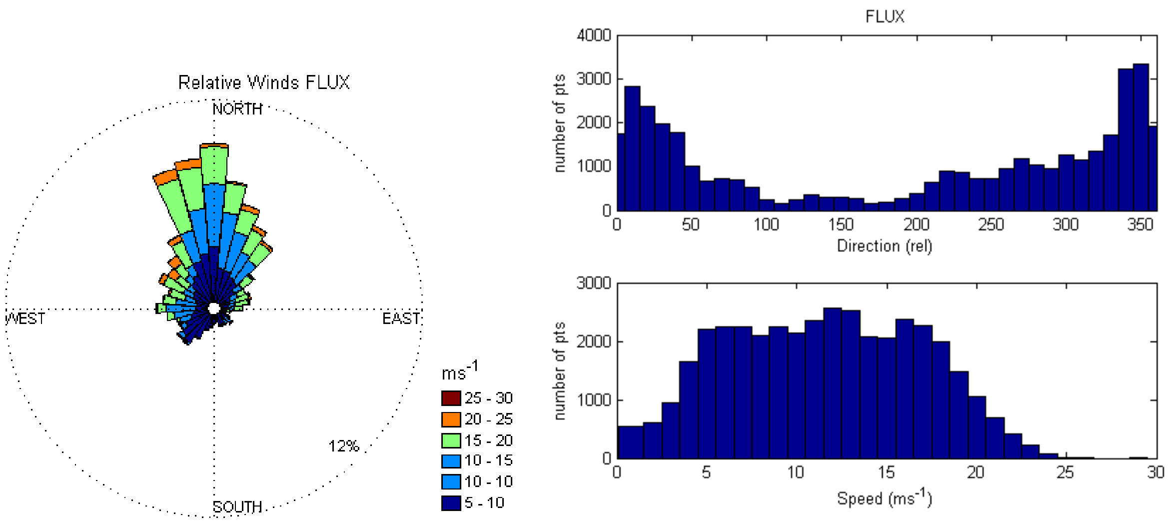

Figure 11. Left side are wind roses for the 3 wind sensors for times when all 3 sensors have data and the right side are histograms for all the data from each sensor. Outer ring represents 12% of total points. All data are 1 min averages.

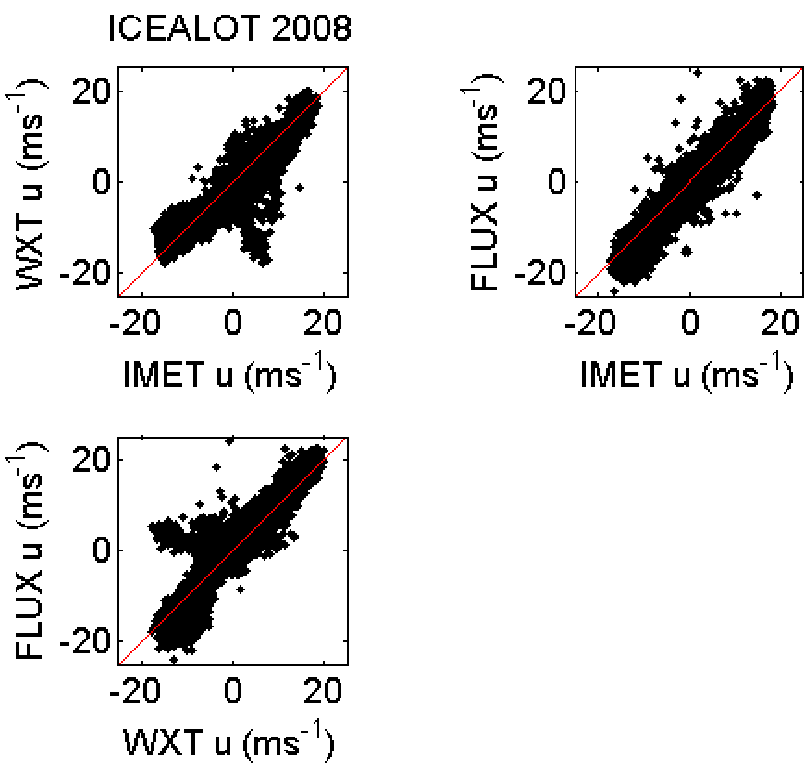

Figure 8. U-component comparisons (u is positive for winds from the bow).

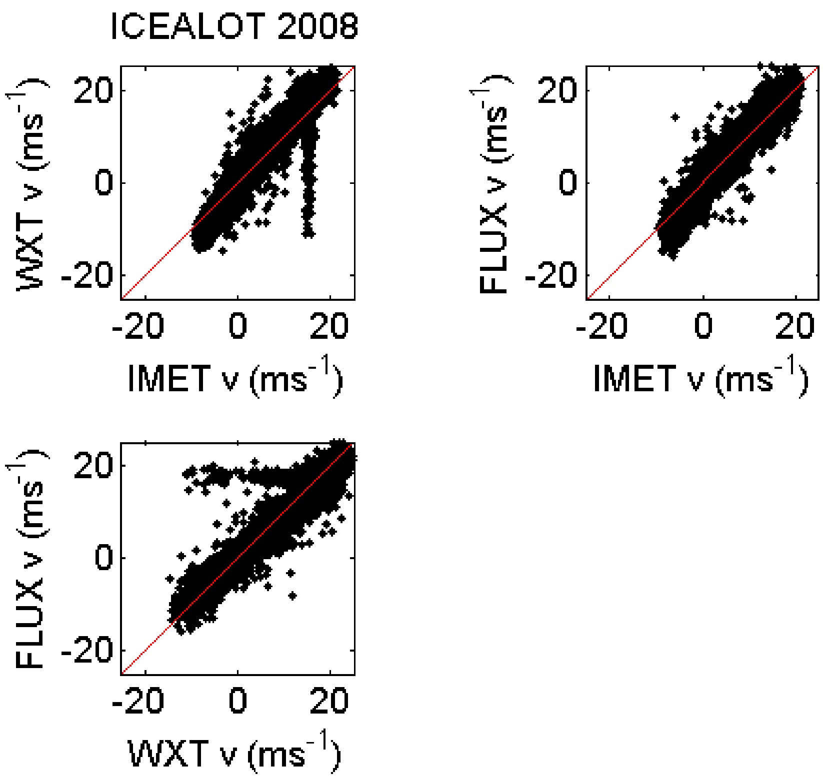

Figure 12. v-component comparisons (v is positive for winds from the starboard).

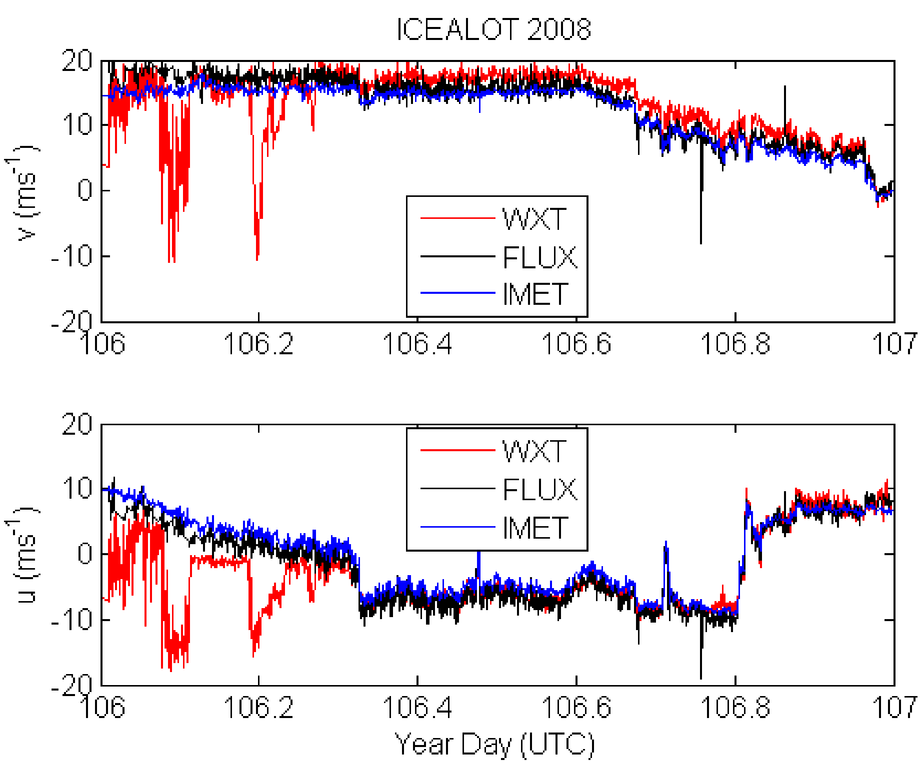

Figure 13. Expanded view of April 15, 2009 (Year Day 106).

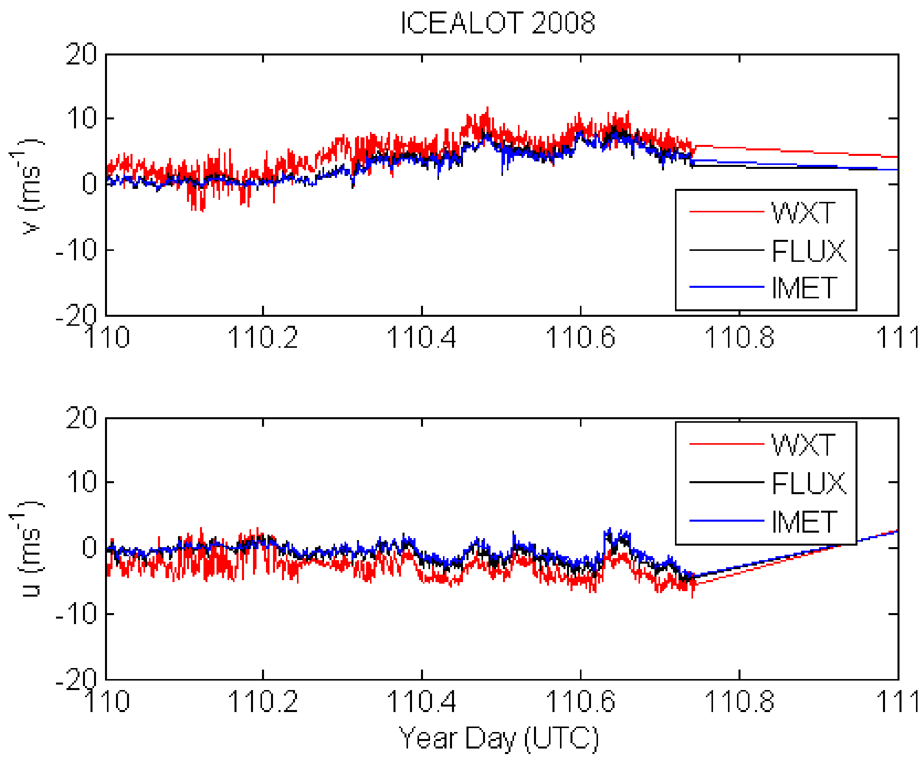

Figure 14. Expanded view of April 20, 2009 (Year Day 110).

Air Temperature and Relative Humidity:

It should be noted that the FLUX sensor is aspirated by a fan while the IMET and WXT rely on the wind for natural ventilation. The relative winds provided by the nearly constant forward motion of the ship (Fig 8) should have provided ample natural ventilation for both the IMET and WXT. The missing data between Year Day 89 and 105 is due to damage to the FLUX system caused by rough seas while crossing the Atlantic. As a result of this damage the FLUX T/RH on Leg1 was replaced by a different T/RH sensor on Leg2.

Figure 15 shows the time series of all 3 sensors and Table 5 lists the statistics and correlations for the air temperature sensors. The comparisons were broken down into Leg 1 and Leg2, because the damage to the FLUX system mentioned above. All three sensors show good agreement and correlation (Table 5 and Fig 16). On Leg 1 the FLUX temperature sensor is showing more scatter compared to the IMET or WXT and is offset high 0.5-1.0^{o}C. For Leg 2 the scatter is less and the offset is about half that of Leg1. The lower right hand scatter plot in Fig 16 is a comparison of the IMET and WXT sensors for the entire cruise, including the period when the FLUX sensor was unavailable. No significant differences are seen by including these data.

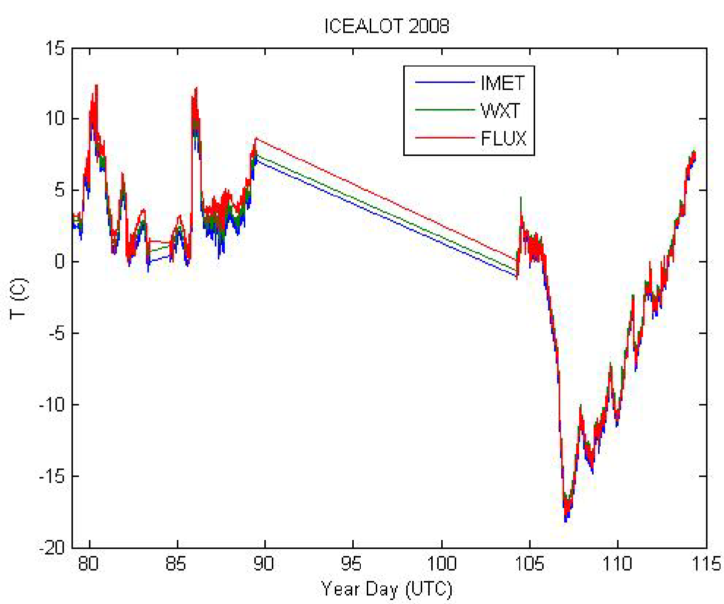

Figure 15. Time series of air temperature from all 3 sensors.

Table 5. T_{air}

	Mean	Min	Max	STD	1 vs 2	1 vs 3	2 vs 3
Leg1							
1. IMET	3.42	-0.74	11.46	2.67	.998	.996	
2. WXT	3.90	0.10	11.80	2.63			.996
3. FLUX	4.56	0.43	12.42	2.58	.996	996	.996
Leg2							
1. IMET	-5.13	-18.25	7.54	6.66	.999	.999	
2. WXT	-4.62	-17.50	7.80	6.56			.999
3. FLUX	-4.90	-17.90	7.67	6.60	.999	.999	.999

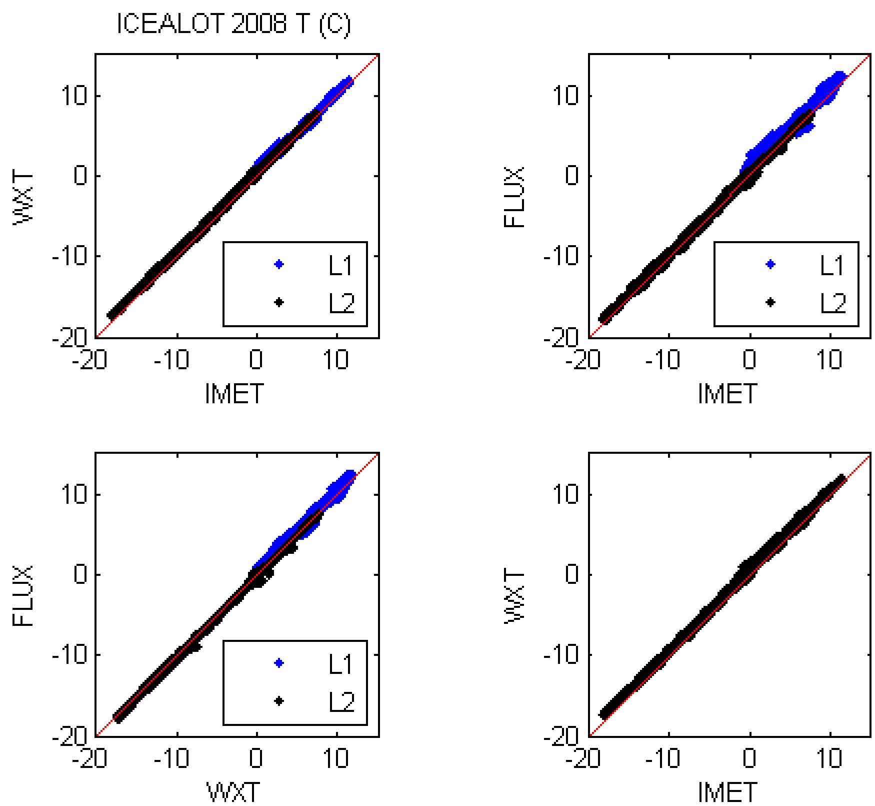

Figure 16. Air Temperature comparison of all 3 sensors. L1 = Leg1 L2 = Leg2

Figure 17 shows the time series of all 3 sensors and Table 6 lists the statistics and correlations for the relative humidity sensors. The comparisons were broken down into Leg 1 and Leg2, because the damage to the FLUX system mentioned above. All three sensors show good agreement and correlation (Table 6 and Fig 18). The FLUX sensor does have a slightly larger STD with temperatures above 0.0^{o}C having a little more scatter which is depicted in Fig. 13. Table 6 lists the statistics and correlations for the relative humidity sensors. Again all three sensors show good agreement and correlation (Table 6 and Fig 14). On Legs 1&2 the FLUX relative humidity sensor is showing a little more scatter compared to the IMET or WXT for relative humidity's above 50%. The WXT on Leg 1 is slightly lower, 2%, than the IMET or

WXT. For Leg 2 this offset increases to 6%. This increased offset correlates to a period of very cold temperatures (Fig 15), but does not change when the temperatures warm. For the last 2-3 days at the very end of the of the cruise the FLUX and IMET sensors show a sudden offset of nearly 10% after tracking within 2% most of Leg 2. This also happens after the cold period. Only the FLUX sensor ever reports a relative humidity of 100% while the IMET and WXT maxed out at 92% and 96% respectively. The lower right hand scatter plot in Fig 18 is a comparison of the IMET and WXT sensors for the entire cruise, including the period when the FLUX sensor was unavailable. No significant differences are seen by including these data.

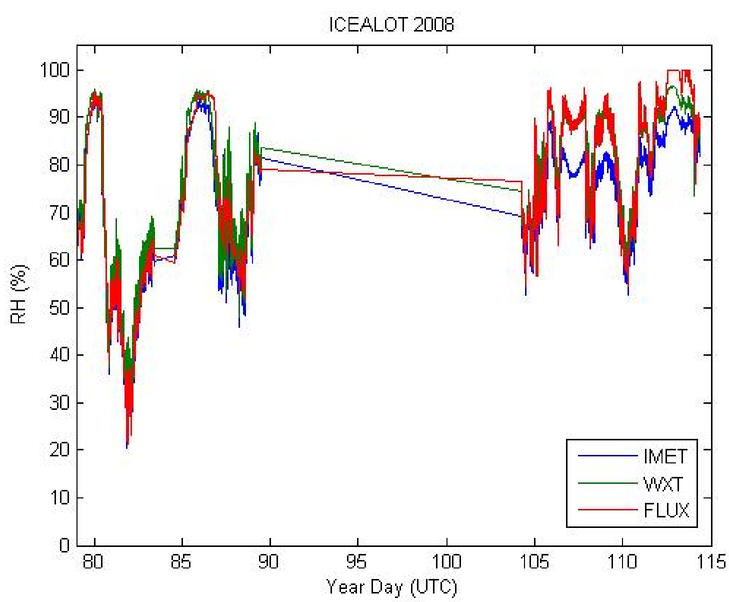

Figure 17. Time series of RH for all 3 sensors.

Table 6. RH

	Mean	Min	Max	STD	1 vs 2	1 vs 3	2 vs 3
Leg1							
1. IMET	68.53	20.33	93.79	17.23	.997	.975	
2. WXT	70.84	22.03	96.00	17.51	.997		.971
3.FLUX	69.16	21.10	95.59	18.14		.975	.971
Leg2							
1. IMET	77.70	52.55	92.34	9.15	.965	.976	
2. WXT	83.71	55.90	96.70	9.85	.965		.986
3. FLUX	83.95	54.35	100.00	11.89		.976	.986

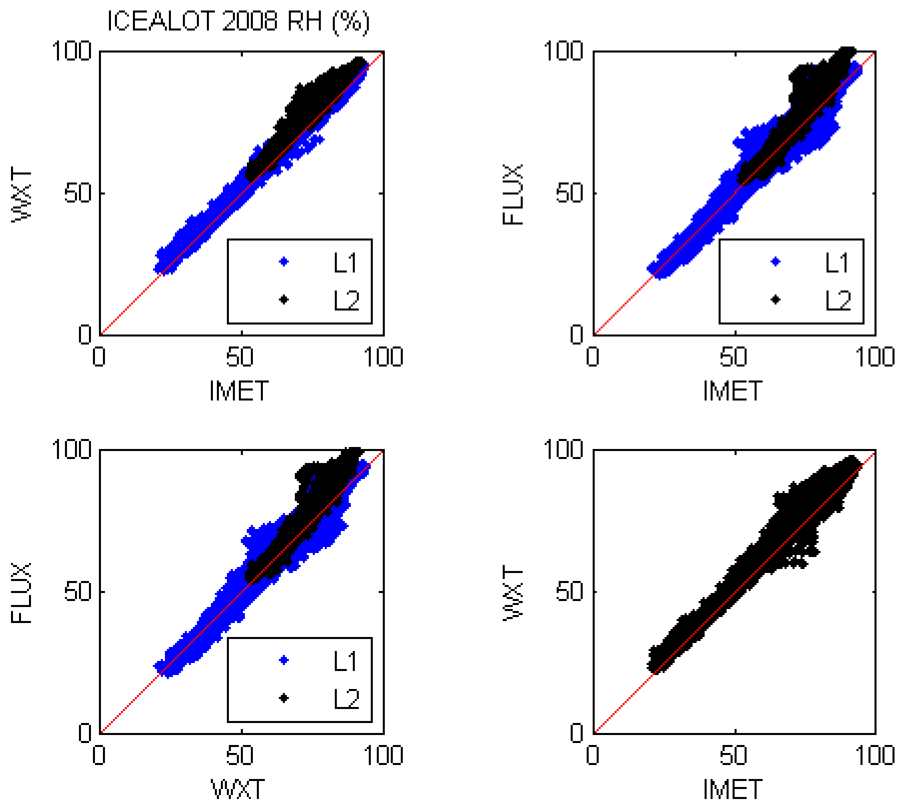

Figure 18. Relative Humidity comparisons. L1 = Leg1 L2 = Leg2

Pressure:

It should be noted that the IMET pressure sensor has a static pressure port to minimize errors due to wind and the WXT sensor does not. For this cruise there was no FLUX pressure sensor. Figures 19&20 are the time series of the two sensors and a scatter plot comparison and Table 7 lists the statistics and correlations for the two pressure sensors. As expected there are only slight differences that can be attributed to sensor accuracies and possibly some wind effects.

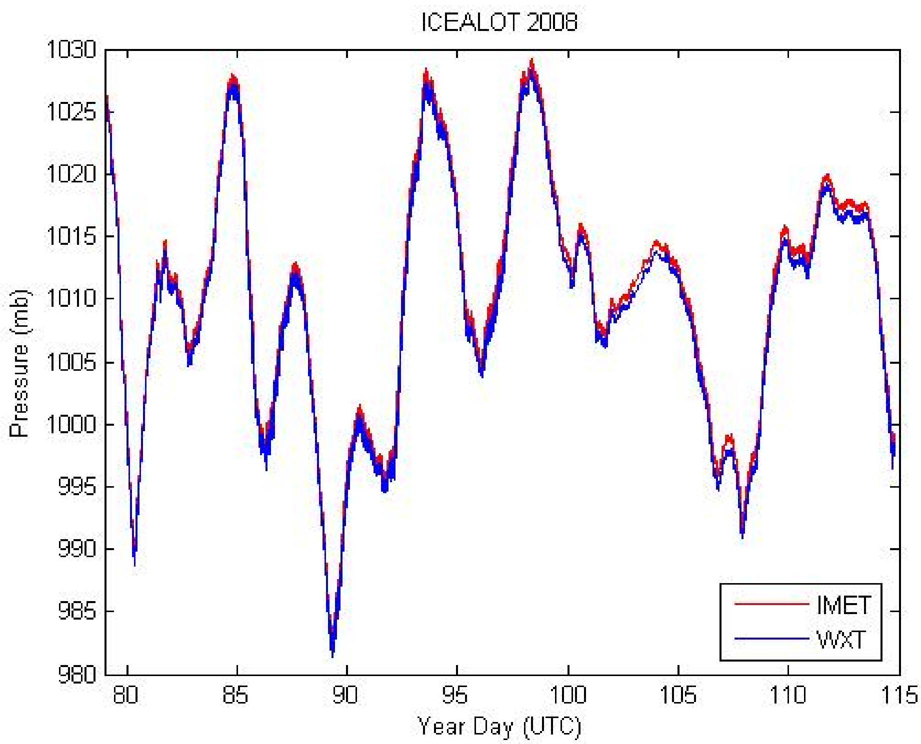

Figure 19. Time series of Pressure for 2 sensors.

Table 7. Pressure:

	Mean	Min	Max	STD	1 vs 2
1 **IMET**	1010.2	981.9	1029.2	9.65	.9996
2 **WXT**	1009.4	981.42	1028.4	9.63	.9996
3 **FLUX**	NA	NA	NA	NA	

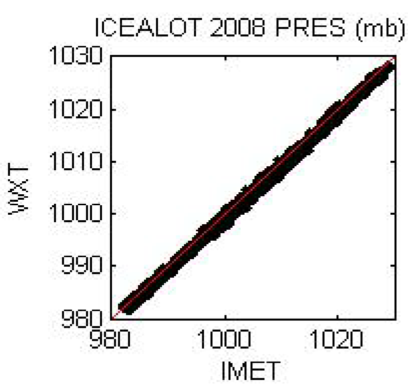

Figure 20. Pressure comparisons.

Short-wave radiation:

It should be noted that the IMET and FLUX short-wave (SW) radiation sensors were not co-located on the forward mast. Figure 1 shows their positions relative to the ship. Both the IMET and FLUX SW sensors are Eppley PSP units (Fig 21), with the IMET package specifically designed for ship and buoy mounting. The FLUX SW location was chosen so that daily cleaning could be carried out. The effects of not being able to clean the IMET sensor are discussed later in this comparison section. Figure 22 shows that the cruise was dominated by cloudy conditions, especially during Leg 2. Table 8 and Figure 23 show the statistics and correlations of the 2 sensors. The most noticeable differences in Table 8 are the mean and maximum values, with the IMET having a larger mean and the FLUX a larger maximum. Both these differences are believed to be a result of how the incoming radiation was affected by the relative positions. Figure 24 shows one of the few clear days and the direct affect of shadowing on the FLUX sensor both early in the morning and late in the day. Overall the scatter seen in Fig. 23 is not as bad as one might expect given the potential for shadowing on the FLUX system. The fact that a location on the ship is constantly changing with respect to the sun means shadowing of the FLUX sensors by the ship's structure is not consistent from day to day. One other factor that had a direct affect on the incoming radiation was the fact that the cruise started out at 40^{o}N reaching 80^{o}N late in the cruise. Figure 24 shows two plots of modeled incoming SW. The top image is at 40^{o}N which shows the length of day doesn't change much, but the maximum increases by approximately 200 Wm^{-2}. At 80^{o}N in the bottom image there is a significant increase in both the length of the day and maximum incoming SW of close to 350 Wm^{-2}. Finally at the higher latitudes the ship encountered periods or riming. Figures 24 shows a cloudy day with no riming and Fig. 25 shows a cloudy day with riming. Figures 26 and 27 are pictures of the type of riming experience in the forward mast (IMET) and mid-ships where the FLUX radiometer was located. April 16 (Year Day 107) was an unusual case with heavy riming on the forward mast and it emphasizes the importance of being able to clean the radiometer dome.

Flux Short-wave radiometer

IMET Short-wave radiometer

Figure 21. FLUX and IMET short-wave radiometers

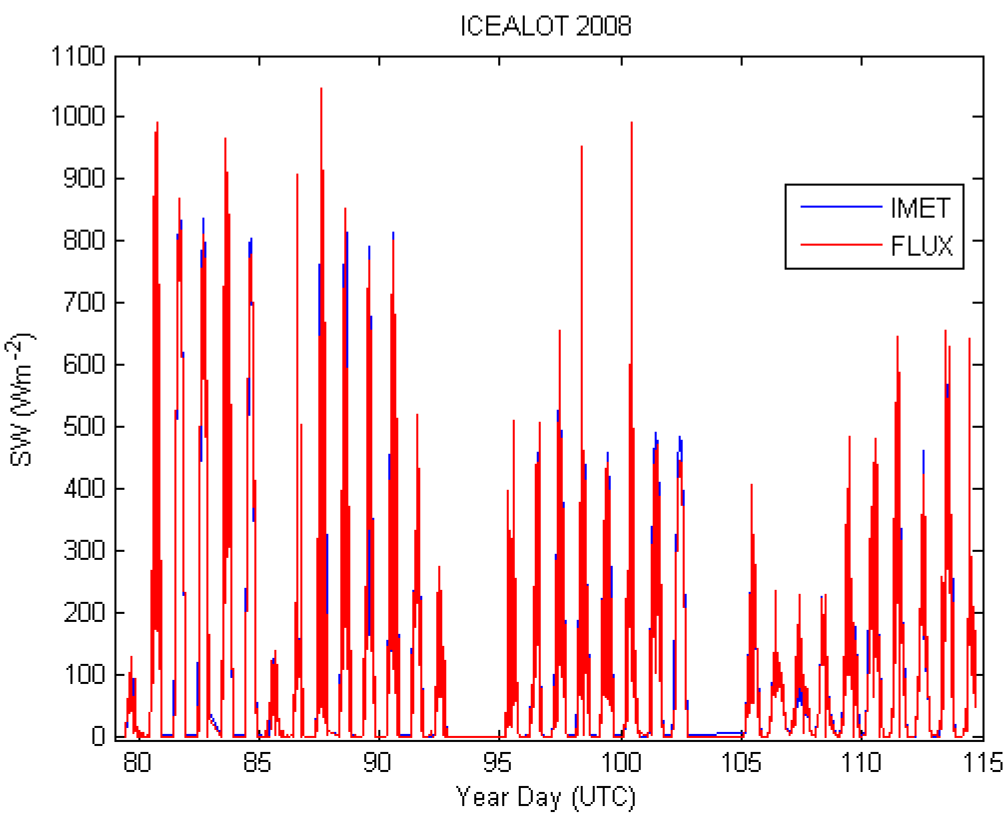

Figure 22. Time series of two short-wave radiometers for entire cruise.

Table 8 SW (Wm^{-2})

	Mean	Min	Max	STD	1 vs 3
1 **IMET**	160.4	-1.5	961.5	189.4	.9822
2 **WXT**	NA	NA	NA	NA	
3 **FLUX**	155.5	0.0	1045.9	191.9	.9822

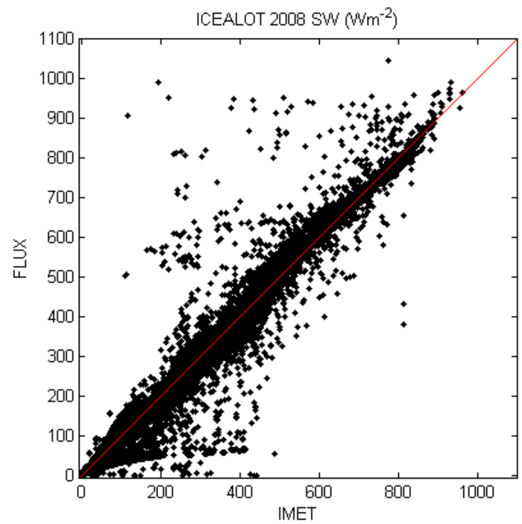

Figure 21. Comparison of IMET and FLUX short-wave solar radiation.

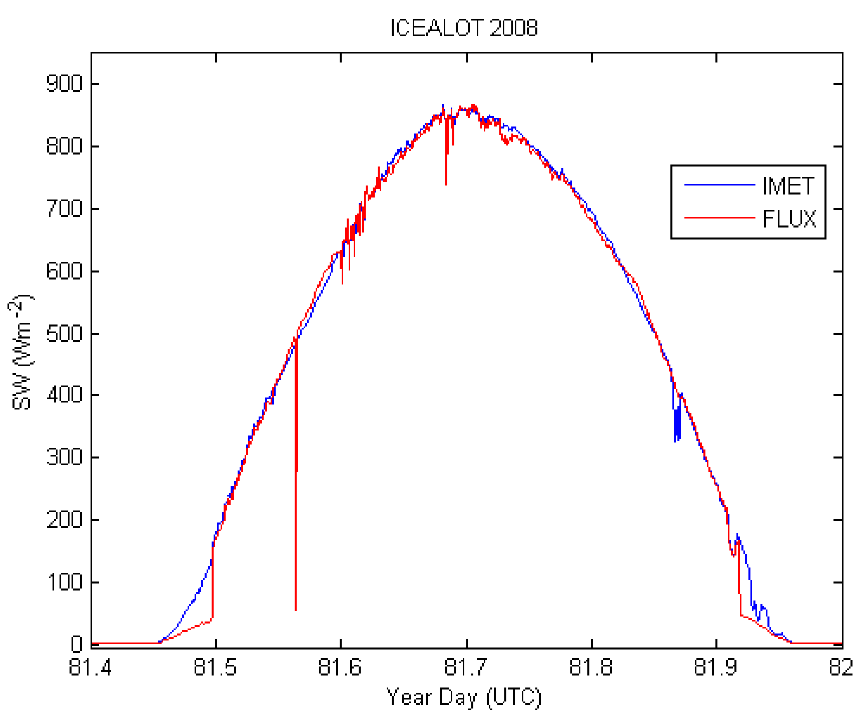

Figure 22. Short-wave solar radiation comparison Mar 21, 2008

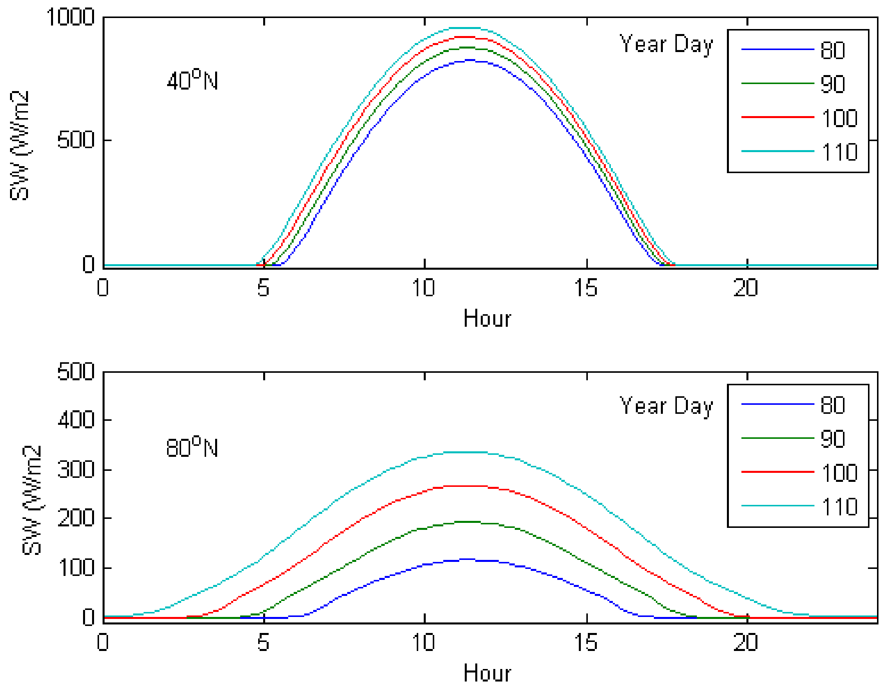

Figure 23. Modeled incoming SW at 40 and 80°N for Year Days 80, 90, 100, 110.

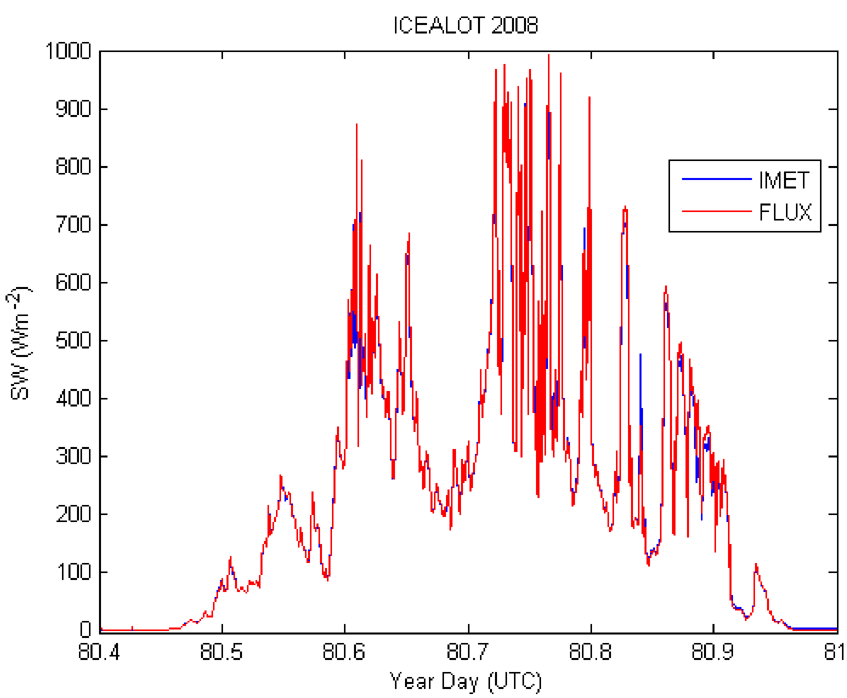

Figure 24. Short-wave solar radiation comparison on March 20, 2008 (Year Day 80).

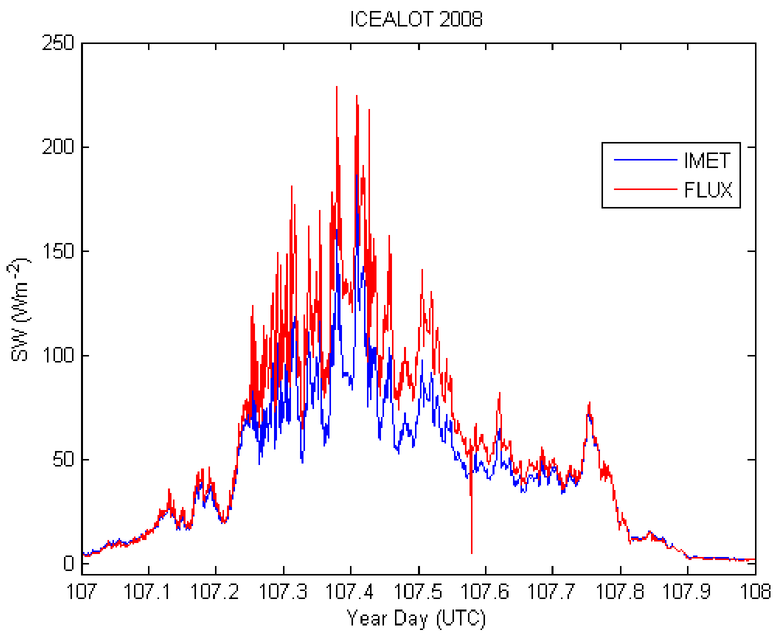

Figure 25. Short-wave solar radiation comparison on April 16, 2008.

Figure 23. Heavy riming on forward mast April 16, 2008 (Year Day 107).

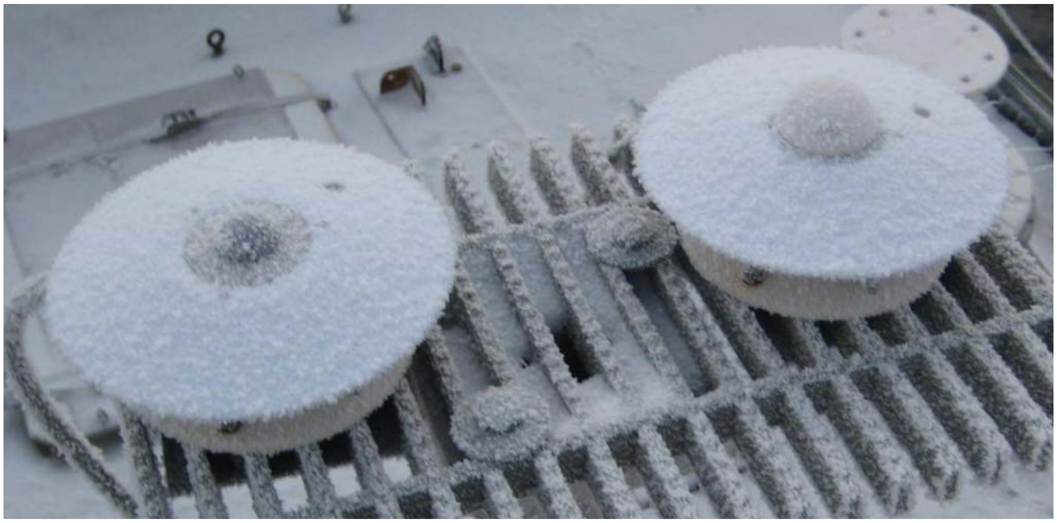

Figure 25. FLUX radiometers on April 16, 2008 (Year Day 107) prior to cleaning.

Precipitation:

There were only 2-3 actual rain events that occurred during Leg 1 and then a couple very small and short snow events during Leg 2. The FLUX precipitation sensor was not working during Leg 2 due to the damage caused by rough seas.

As mentioned earlier there are very different measurement techniques used by the three sensors. The IMET rain gauge is heated and uses an automatic siphoning technique designed for use on ships and buoys because there are no moving parts in a tipping-bucket rain gauge. The WXT rain gauge uses the acoustic intensity of rain drops striking the sensor with larger drops correlating to larger acoustic intensity. The FLUX optical rain gauge uses variations in the light intensity measured as precipitation falls through the optical path. All three sensors can report rain rate and accumulation. The IMET unit automatically drains after 50 mm of total accumulation. Figure 3 shows that the IMET and WXT units were mounted right next to each other as high as possible on the tower. Figures 25 and 26 show the rain accumulation and rain rate for March 20, 2008 (Year Day 80). There is very good agreement with the start of each of the four rain events and the total accumulation (~4.5mm) for this day, but the amounts for the individual rain events or steps vary at times by as much as 100%. A second day (Figs. 26 & 27) with a larger total accumulation shows the WXT and FLUX agreeing, while the IMET total is low by a factor of three. The IMET only has a resolution of 1mm compared to the WXT and FLUX of 0.01 and 0.001 mm respectively. As reported by Nystuen et al. 1996 the IMET is best above 5 $mmhr^{-1}$. Figures 29 & 30 show comparisons of total accumulation on 9 days. Comparing the relative winds (not shown) to the rain events there are three somewhat distinct patterns. Year Day 80 winds are 5-6 ms^{-1} and predominately bow on. Year Day 85 has much stronger winds, (20 ms^{-1}) and with winds both bow on for the first event and slightly from the starboard aft. Year Day 86 the winds are 12 ms^{-1} and again from the starboard aft. Lower IMET accumulation totals (Fig. 29) are consistent with findings by Bradley et al., 2004.

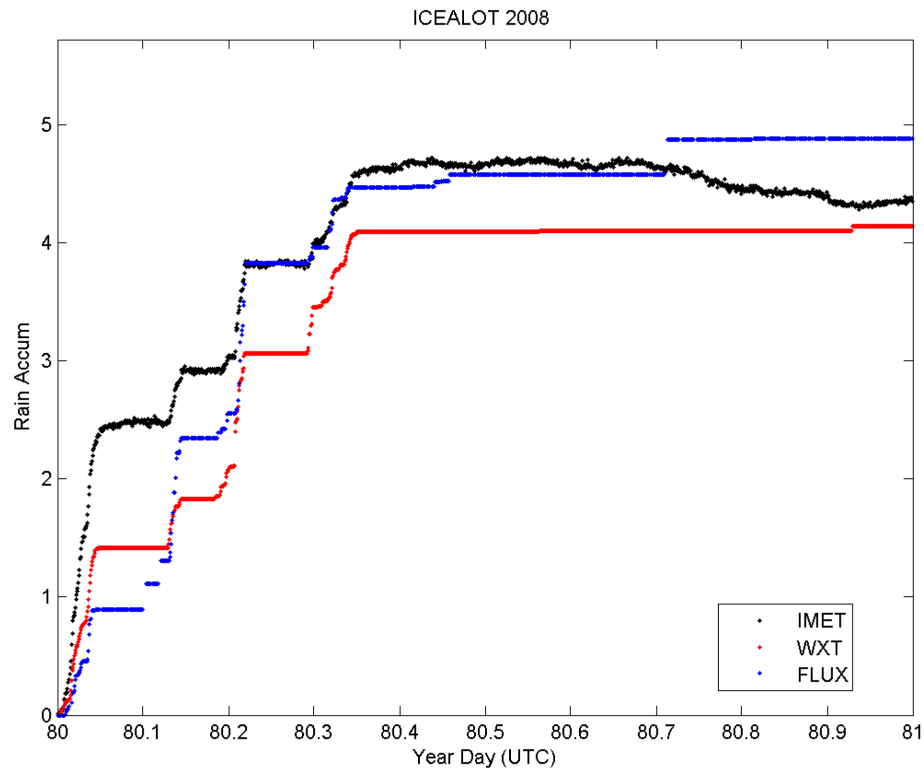

Figure 25. Total rain accumulation for March 20, 2008.

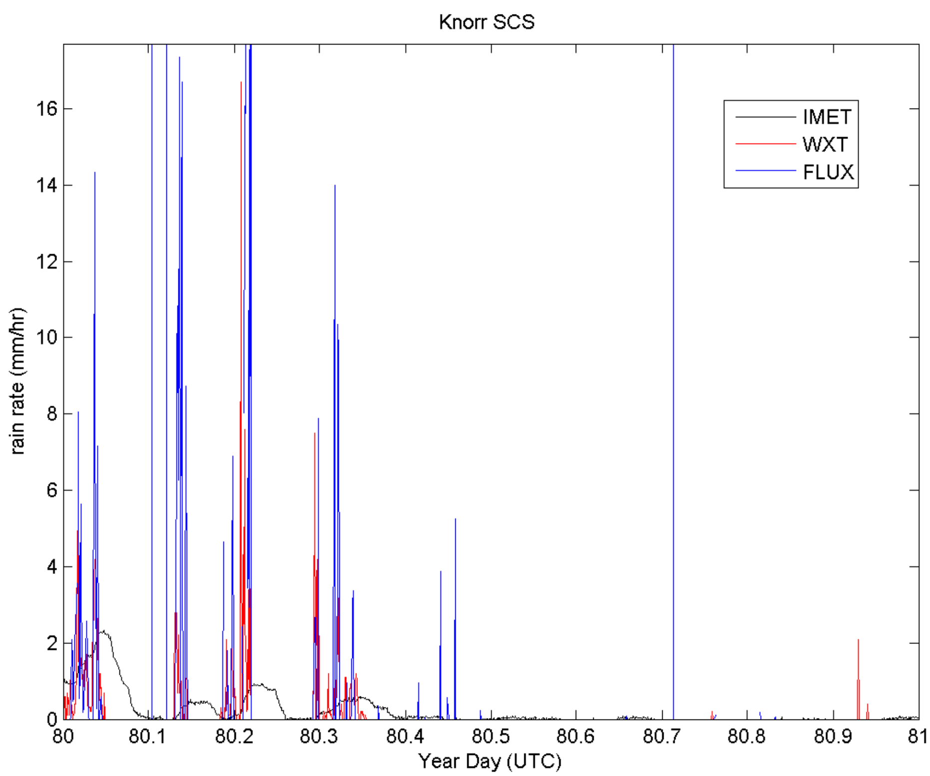

Figure 25. Rain rate for March 20, 2008.

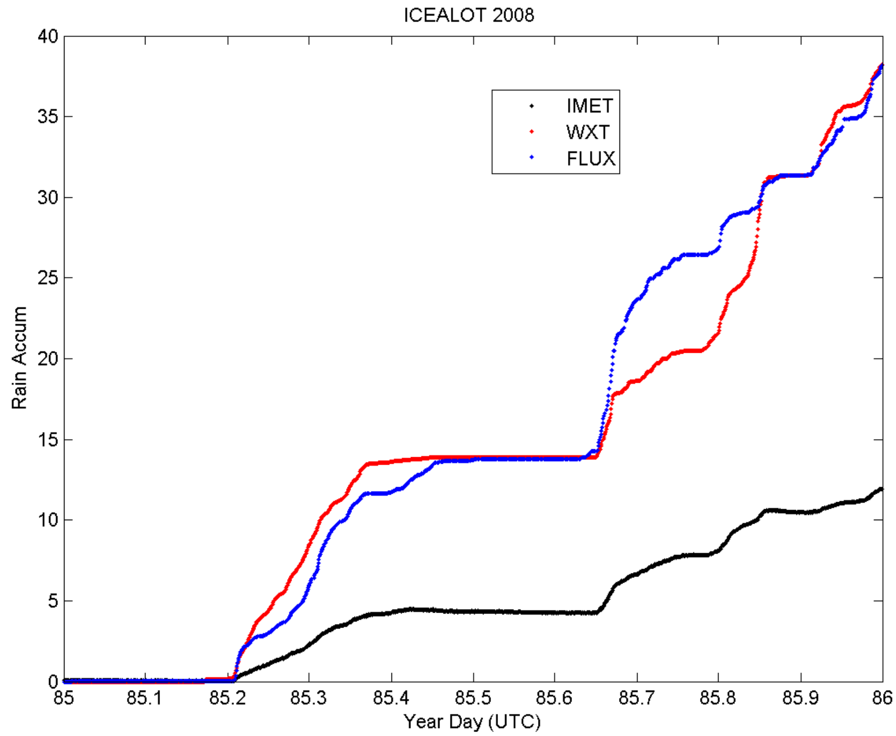

Figure 26. Total rain accumulation for March 25, 2008.

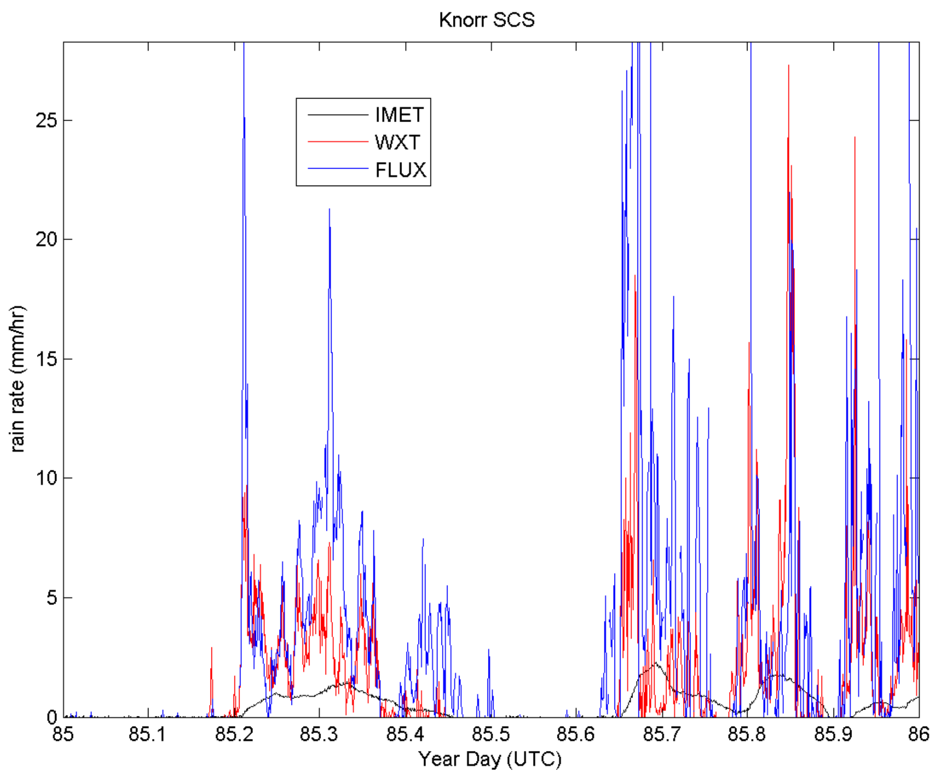

Figure 27. Rain rate for March 25, 2008.

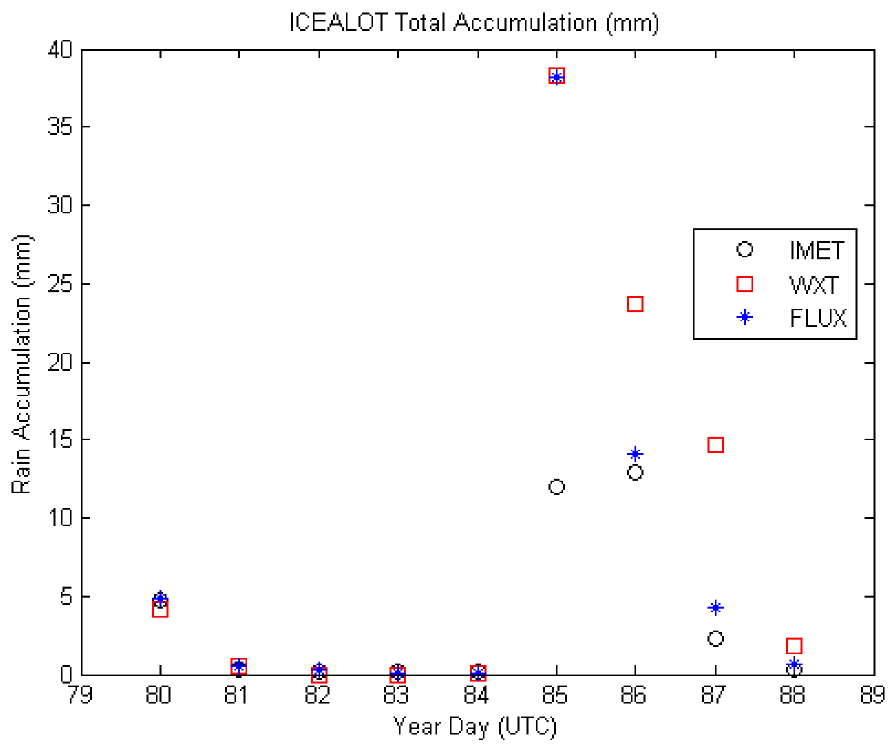

Figure 29. Daily rain totals (mm) for 9 days on Leg 1.

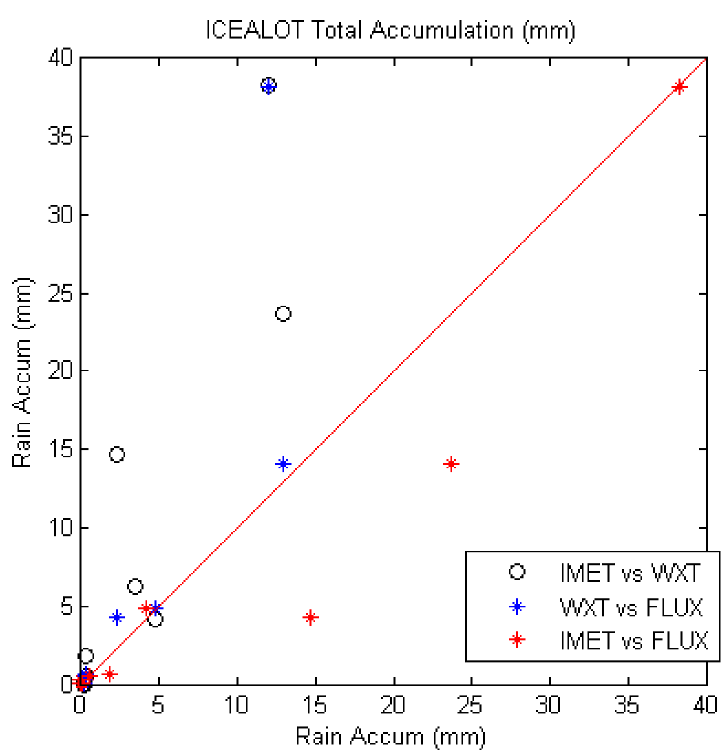

Figure 30. Comparisons of rain totals (mm) for 9 days on Leg 1.

Summary:

There were 3 sets of sensors collecting meteorological data during ICEALOT. The IMET is the system currently operating on most research vessels. The WXT system was being tested as a possible replacement to the IMET due to its reduced cost and the maintenance required. The FLUX system is the portable flux standard used for comparison and calibration. Conditions during ICEALOT included very rough seas and strong winds and cold, snow, and riming above the Arctic Circle. Except for the incoming SW radiation, the sensors were all mounted on the forward mast (Fig. 3).

- Wind comparisons show consistency between sensors with the IMET wind speeds reading lower that the IMET and FLUX. Detailed analysis of the WXT data found periods of increased variability and offsets in the speed and direction. Further comparisons are needed to determine if these differences are related to the mechanical vs. acoustic measurement techniques and possible initial sensor alignment errors. Based on this limited data set the WXT wind sensor is not recommended for cold Arctic like conditions.
- Temperature comparisons show very good agreement with small differences most likely associated with sensor accuracies.
- The three RH sensors have fairly significant differences in accuracy, especially at higher humidity’s. This explains some of the larger offsets but not why the maximum reading of these sensors differed by as much as 8% at the high end with only the FLUX sensor ever reading 100%.
- Results for the IMET and FLUX incoming solar radiation are consistent with what is expected for two sensors mounted in different locations on the ship: one with daily maintenance (FLUX) and one without (IMET). Deciding how much sensor location will compromise the data or make quality control difficult is important and should be taken into serious consideration prior to the start of any field campaign.
- Due to the limited number of precipitation events, no final conclusion can be made from the precipitation sensor comparisons. What comparisons there are, are consistent with previous findings that optical rain gauges, similar to the FLUX, do a god job while the IMET siphon gauges have proven to seriously underestimate in strong winds. The WXT unit is basically an acoustic disdrometer. Previous tests using disdrometers on ships have not shown promise.

REFERENCES:

Fairall, C.W., 1991: The humidity/temperature sensitivity of clear-air radars in the convective boundary layer. J. Appl. Meteor. 30, 1064-1074.

Fairall, C.W., J. Kepert, and G.J. Holland, 1995: The effect of sea spray on surface energy transports over the ocean. The Global Atmospheric Ocean System, 2, 121-142.

Fairall, C.W., E.F. Bradley, D.P. Rogers, J.B. Edson, and G.S. Young, 1996: Bulk parameterization of air-sea fluxes for TOGA COARE. J. Geophys. Res.,101, 3747-3767.

Fairall, C.W., A. B. White, 1997: J. B. Edson, and J. E. Hare. Integrated Shipboard Measurements of the Marine Boundary Layer, 1997: *Journal of Atmospheric and Oceanic Technology* Volume 14, Issue 3 pp. 338–359 DOI: 10.1175/1520-0426(1997)014<0338:ISMOTM>2.0.CO;2

Fairall, C. W., J. E. Hare, J. B. Edson, and W. McGillis, 2000: Parameterization and Micrometeorological Measurement of Air-Sea Gas Transfer. *Bound.-Layer Meteor*., Vol 96, pp 63-105.

Fairall, C.W., Taneil Uttal, Duane Hazen, Jeffrey Hare, Meghan F. Cronin, Nicholas Bond, and Dana E. Veron , 2008: Observations of Cloud, Radiation, and Surface Forcing in the Equatorial Eastern Pacific *Journal of Climate* , Volume 21, Issue 4 pp. 655–673.

Hosom, D.S., Robert A. Weller, Richard E. Payne, and Kenneth E. Prada, 1995: The IMET (Improved Meteorology) Ship and Buoy Systems, *Journal of Atmospheric and Oceanic Technology* Volume 12, Issue 3 pp. 527–540.

Nystuen, J.A., John R. Proni, Peter G. Black, and John C. Wilkerson. A Comparison of Automatic Rain Gauges, 1996: *Journal of Atmospheric and Oceanic Technology* , Volume 13, Issue 1 pp. 62–73.

Weller, R.A., Frank Bradley, and Roger Lukas . The Interface or Air–Sea Flux Component of the TOGA Coupled Ocean–Atmosphere Response Experiment and Its Impact on Subsequent Air–Sea Interaction Studies, 2004: *Journal of Atmospheric and Oceanic Technology*, Volume 21, Issue 2 pp. 223–257.

White, A.B., C.W. Fairall, and J.B. Snider, 1995: Surface-based remote sensing of marine boundary layer cloud properties. J. Atmos. Sci., 52, 2827-2838.